Mars' Surface Radiation Environment Measured with the Mars Science Laboratory's Curiosity Rover

Donald M. Hassler,[1]* Cary Zeitlin,[1] Robert F. Wimmer-Schweingruber,[2] Bent Ehresmann,[1] Scot Rafkin,[1] Jennifer L. Eigenbrode,[3] David E. Brinza,[4] Gerald Weigle,[5] Stephan Böttcher,[2] Eckart Böhm,[2] Soenke Burmeister,[2] Jingnan Guo,[2] Jan Köhler,[2] Cesar Martin,[2] Guenther Reitz,[6] Francis A. Cucinotta,[7] Myung-Hee Kim,[8] David Grinspoon,[9] Mark A. Bullock,[1] Arik Posner,[10] Javier Gómez-Elvira,[11] Ashwin Vasavada,[4] John P. Grotzinger,[4] MSL Science Team†

The Radiation Assessment Detector (RAD) on the Mars Science Laboratory's Curiosity rover began making detailed measurements of the cosmic ray and energetic particle radiation environment on the surface of Mars on 7 August 2012. We report and discuss measurements of the absorbed dose and dose equivalent from galactic cosmic rays and solar energetic particles on the martian surface for ~300 days of observations during the current solar maximum. These measurements provide insight into the radiation hazards associated with a human mission to the surface of Mars and provide an anchor point with which to model the subsurface radiation environment, with implications for microbial survival times of any possible extant or past life, as well as for the preservation of potential organic biosignatures of the ancient martian environment.

The radiation exposure on the surface of Mars is much harsher than that on the surface of the Earth for two reasons: Mars lacks a global magnetic field to deflect energetic charged particles ([1]), and the martian atmosphere is much thinner (<1%) than that of Earth, providing little shielding against the high-energy particles that are incident at the top of its atmosphere. This environmental factor, for which there is no analog on Earth, poses a challenge for future human exploration of Mars ([2–9]) and is also important in understanding both geological and potential biological evolution on Mars. The radiation environment on Mars has been previously estimated and modeled ([10–17]). Here, we report in situ measurements of the ionizing radiation environment on the surface of Mars; these can be used to test and validate radiation transport models.

There are two types of energetic particle radiation incident at the top of the Mars atmosphere, galactic cosmic rays (GCRs) and solar energetic particles (SEPs). Both GCRs and SEPs interact with the atmosphere and, if energetic enough, penetrate into the martian soil, or regolith, where they produce secondary particles (including neutrons and γ-rays) that contribute to the complex radiation environment on the martian surface, which is quite unlike that observed at the Earth's surface.

GCRs are high-energy particles [10 megaelectron volt per nuclear particle (MeV/nuc) to >10 GeV/nuc], fluxes of which are modulated by the heliosphere and anticorrelated with solar activity ([18]). The composition varies slightly depending on solar modulation, with the proton abundance in the range of 85 to 90%, helium ions ~10 to 13%, electrons ~1%, and ~1% heavier nuclei ([19], [20]). Because of their high energies, GCRs are difficult to shield against and can penetrate up to several meters into the martian regolith. SEPs are produced in the solar corona as a result of high-energy processes associated with flares, coronal mass ejections (CMEs), and their corresponding shocks. SEP events are sporadic and difficult to predict, with onset times on the order of minutes to hours and durations of hours to days. SEP fluxes can vary by several orders of magnitude and are typically dominated by protons, but composition can vary substantially ([21]). SEP protons and helium ions with energies below ~150 MeV/nuc ("soft" spectrum events) do not penetrate to the martian surface. Typical column depths of the martian atmosphere at Gale crater are on the order of 20 g/cm^2, thus energetic particles with energies less than ~150 MeV lose all of their energy before passing through this amount of material. However, during "hard spectrum" events ions can be accelerated to energies well above 150 MeV/nuc, with substantial fluxes reaching the martian surface. In all events, secondary neutrons produced by SEPs in the atmosphere can reach the surface. The Radiation Assessment Detector (RAD) measurements reported here cover observations of GCRs as well as hard and soft SEP events seen from the martian surface. Together with the radiation environment results from RAD inside the Mars Science Laboratory (MSL) spacecraft during its cruise to Mars ([22]), these measurements correspond to all three phases (outbound interplanetary journey, Mars surface stay, and return journey) of a human Mars mission at this time in the solar cycle and thus are directly relevant to planning for future human missions.

If martian life exists, or existed in the past, it is reasonable to assume it is or was based on organic molecules ([23], [24]) and will therefore share with terrestrial life the vulnerability to energetic particle radiation ([25], [26]). Thus, we present here extrapolations of the RAD surface dose measurements (using transport models) to the martian subsurface, with implications for estimating lethal depths and microbial survival times ([26–30]). The radiation environment on Mars may also play a key role in the chemical alteration of the regolith and martian rocks over geologic time scales, affecting the preservation of organics, including potential organic biosignatures of the ancient martian environment ([26], [27]). The RAD surface measurements provide a baseline for inferring the flux in these more shielded environments (by validating and anchoring transport models) and thus the foundation for understanding the limits to preservation of organic matter in the soil and rocks of Gale crater.

Results and Discussion

The Curiosity rover landed successfully on Mars in Gale crater at ~–4.4 km MOLA (Mars Orbiter Laser Altimeter) altitude on 6 August 2012. On 7 August 2012, the RAD began taking observations of the radiation environment on Mars, incidentally 100 years to the day after the discovery of cosmic rays on Earth by Victor Hess from a balloon in Austria ([31]). The results reported here are time series of absorbed dose rate, the average absorbed dose rate and average dose equivalent rate, and Linear Energy Transfer (LET) spectra for ~300 sols (1 martian sol = 24 hours 39 min.) from 7 August 2012 to 1 June 2013.

The radiation dose rate measured by RAD on the Mars surface during the first 300 sols on Mars is shown in Fig. 1, near the maximum of solar cycle 24. The GCR dose rate can be seen to vary between 180 and 225 microgray (μGy)/day, owing to the combined effects of diurnal variations from atmospheric pressure changes, Mars seasonal variations at Gale crater, and heliospheric structure variability due to solar activity and rotation.

The diurnal dose rates vary by a few percent because of diurnal change in the Mars atmospheric column, as can be seen in Fig. 2A, which shows data obtained between sols 290 and 302. This

[1]Southwest Research Institute, Boulder, CO 80302, USA. [2]Christian Albrechts University, 24118 Kiel, Germany. [3]NASA Goddard Space Flight Center, Greenbelt, MD 20771, USA. [4]Jet Propulsion Laboratory, California Institute of Technology, Pasadena, CA 91109, USA. [5]Southwest Research Institute, San Antonio, TX 78238, USA. [6]German Aerospace Center (DLR), 51147 Cologne, Germany. [7]University of Nevada Las Vegas, Las Vegas, NV 89154, USA. [8]Universities Space Research Association, Houston, TX 77058, USA. [9]Denver Museum of Nature and Science, Denver, CO 80205, USA. [10]NASA Headquarters, Washington, DC 20546, USA. [11]Centro de Astrobiología (INTA-CSIC), 28850 Madrid, Spain.

*Corresponding author. E-mail: hassler@boulder.swri.edu
†MSL Science Team authors and affiliations are listed in the supplementary materials.

diurnal variation of the total atmospheric column mass is related to the daily thermal tides that Mars experiences each sol, by which the direct heating of the martian atmosphere by the Sun produces global-scale waves that redistribute atmospheric mass (33). Comparison of the RAD dose rate to the Rover Environment Monitoring Station (REMS) (34) atmospheric pressure measurements shows there is an anticorrelation between total dose rate and atmospheric pressure (Fig. 2B), which in turn is directly related to column depth.

On the Mars surface, during the 300-day period near the maximum of solar cycle 24, we found an average total GCR dose rate at Gale crater (−4.4 km MOLA) of 0.210 ± 0.040 mGy/day, compared with 0.48 ± 0.08 mGy/day measured during cruise inside the MSL spacecraft (Fig. 3 and Table 1). The difference in dose rate is driven by several influences: First, the shielding of the lower hemisphere provided by the planet reduces the dose rate by a factor of ~2. Second, further deviations from this factor of two are due to interactions of primary GCRs with the nucleons in the atmosphere (and soil). Additionally, the effective atmospheric shielding is thicker than the spacecraft shielding of the instrument during cruise. The dose rate is also influenced by the modulation of the GCR flux by the sun—a stronger solar modulation results in overall lower GCR fluxes and thus lower dose rates. The solar modulation parameter during the surface mission to date has been ~577 MV, whereas the average Φ during cruise was ~635 MV (resulting in lower effective GCR flux).

We find the average quality factor <Q> on the martian surface to be 3.05 ± 0.3, compared with 3.82 ± 0.3 measured during cruise. This smaller <Q> is due to the thicker shielding in the field of view (FOV) on the surface because during cruise, approximately half of the RAD FOV was lightly shielded (< 10 g/cm^2) (35). The column depth of the martian atmosphere averaged about 21 g/cm^2 over the first 300 sols of Curiosity's mission. Combining the tissue dose rate measurement with <Q> yields an average GCR dose-equivalent rate on the Mars surface of 0.64 ± 0.12 millisieverts (mSv)/day (Fig. 4).

The SEP dose was obtained by subtracting the average GCR dose rate for the duration of the SEP event. It was found to be 50 µGy in the less-shielded of the two detectors used for dosimetry. Because the composition of SEP events (observed both on the surface and during cruise) are dominantly protons, for which <Q> = ~1, the dose equivalent from this event was ~50 µSv, approximately equal to 25% of the GCR dose equivalent for the 1-day duration of the event.

The frequency and intensity of SEP events is highly variable and still unpredictable, and although these observations were made near solar maximum, this current solar activity cycle is very weak by historical norms (36). Substantial SEP events throughout recent history (such as February 1956, August 1972, and September 1989) have been reported and modeled to be several orders of magnitude more intense than those currently observed to date by the RAD (37).

Implications for Future Human Missions to Mars

Combining our measurements with those obtained during the cruise phase (22), we estimate a total mission dose equivalent of ~1.01 Sv for a round trip Mars surface mission with 180 days (each way) cruise, and 500 days on the martian surface for this current solar cycle (Table 2). These mission phase durations are based on one possible NASA design reference mission (38); many mission designs and many mission windows at different times in the solar cycle or a different solar cycle would result in somewhat different radiation exposures. Because GCR flux is modulated by solar activity (decreasing during solar activity maximum and increasing during solar activity minimum) and the risk for exposure to SEPs increases with solar activity, the contribution of each to the total mission dose of a future Mars mission depends on when in the solar cycle the mission occurs (3–6).

Estimates of Subsurface Dose Rates

The dose and dose-equivalent rates reported in Tables 1 and 2 can be extrapolated to obtain rates

Fig. 1. Time series of radiation dose rate measured by RAD on the surface of Mars. During this time, RAD observed a dose rate enhancement from one hard SEP event on sol 242 (12 to 13 April 2013) and several Forbush decreases (32), resulting from soft SEP event-related interplanetary coronal mass ejections (ICMEs) on sols 50, 97, 208, and 259. (These ICMEs serve as magnetic shields against the GCR, thus reducing the observed flux.) Occasional brief gaps can also be seen, usually caused by RAD having been powered off so that other activities could take place on the spacecraft without interference.
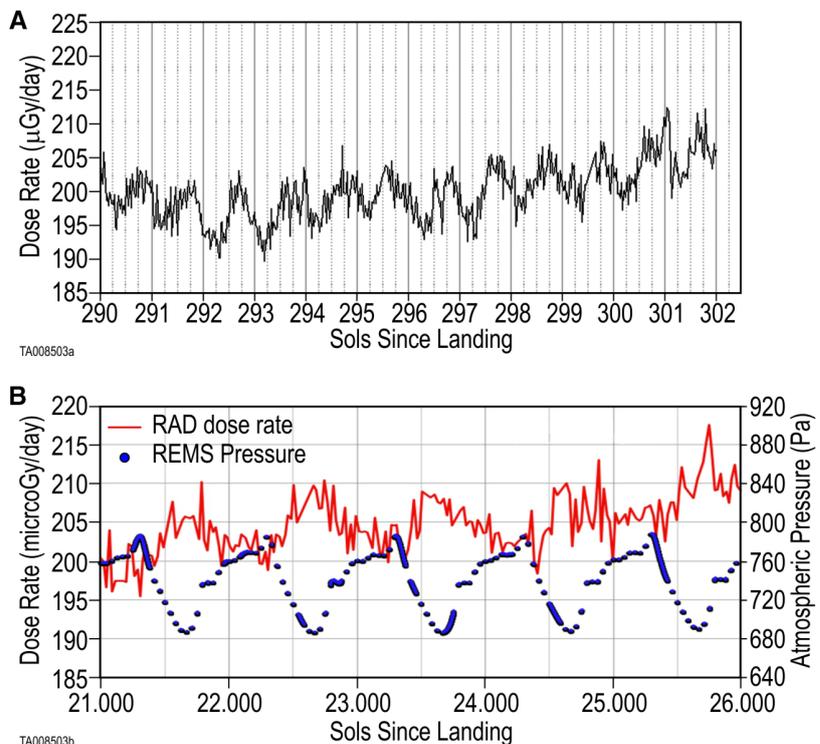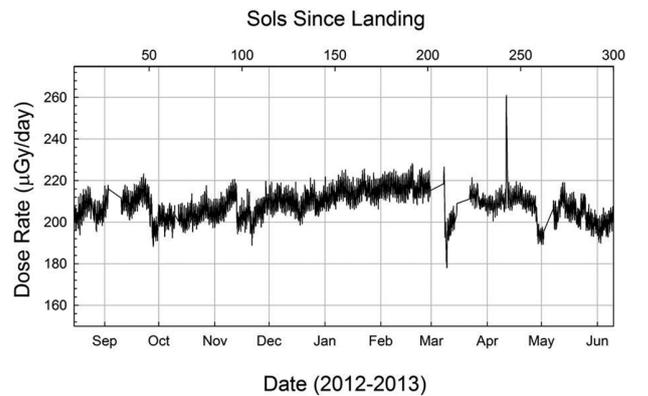

Fig. 2. Comparison of RAD dose rate versus time and atmospheric pressure. (A) RAD daily dose rate versus time. (B) Comparison of RAD dose rate with REMS atmospheric pressure.

below the martian surface by using the surface measurements to anchor model predictions. Refining estimates of the subsurface radiation environment is important because in situ regolith-based materials are prime candidates for astronaut shelter shielding materials in order to reduce or mitigate the biological hazards associated with radiation exposures on future long-duration human missions. These improved subsurface radiation estimates give insight into the potential for the preservation of possible organic biosignatures as a function of depth as well as survival times of possible microbial or bacterial life forms left dormant beneath the surface.

Several studies have modeled the expected subsurface radiation regime (26, 39), but the dose values depended until now on the modeled radiation environment on the surface. Dartnell *et al.* (26, 27) assumed an absorbed dose of ~150 mGy/year at the martian surface, whereas Pavlov *et al.* (28, 29) assumed an absorbed dose of 50 ± 5 mGy/year. The actual absorbed dose measured by the RAD (76 mGy/year at the surface) (Table 3) allows for more precise estimations of the subsurface dose. Differences may be in part due to differing assumptions in the models about the level of solar modulation compared with the

actual level during the measurement period as well as the amount of atmospheric shielding above the surface. Also, all of the above models must assume a rock, ice, or soil density. On the basis of compositional and morphological observations of the rocks at the John Klein site in Gale crater (42), we estimate a rock density of 2.8 g/cm^3, which approximates the density of an iron-rich mudstone or siltstone. Although our estimates of subsurface dose depend strongly on the models we used, they are useful for comparison purposes. The natural background radioactivity on present-day Mars is thought to be on the order of ~1 μGy/day (43), suggesting that GCR radiation is no longer the dominant source of radiation below ~3 m. This also implies that the effectiveness of regolith-based shielding materials no longer improves beyond a thickness of ~3 m.

Implications for Microbial Survival Times

Energetic particles ionize molecules along their tracks. The energy deposited by ionization or excitation greatly exceeds that required to break many molecular bonds—including those in DNA, other organic molecules, and water—thus, ionizing radiation is extremely damaging to biomolecules through both direct and indirect mechanisms. Thus, measurements of the surface and subsurface radiation environment are critical for estimating the survival probability and survival times of possible dormant life forms found in the martian soil, regolith, rock, and ice. For this, the dose rates can be used to calculate the time it would take for different bacterial species to accumulate a lethal dose of radiation in different subsurface depths (44).

Even the radioresistant organism *D. radiodurans* would, if dormant, be eradicated in the top several meters in a time span of a few million years (28, 29). However, inferred recurring climate changes in the post-Noachian era, due to variations in the planetary obliquity on time scales of several hundred thousand to a few million years (45), could lead to recurring periods of metabolic activity of these otherwise dormant life forms. In this case, it is hypothesized that accumulated radiation damages could be repaired, and the "survival clock" of such life forms could be reset to zero for the next dormant phase (26, 28), which could in turn lead to possible survival to present times. It has been (27) estimated that a 2-m-depth drill was necessary to access viable radioresistant cells that may have gone through this reanimation step within 450,000 years. Applying the RAD dose results, we estimate that only a 1-m-depth drill is necessary to access the same viable radioresistant cells.

Implications for the Preservation of Environmental Records and Organic Biosignatures

Whether the bulk of the martian atmosphere was lost before the Noachian era (~3.7 to 4.0 billion years ago), as recent isotope ratio measurements by Curiosity suggest (46), or toward the
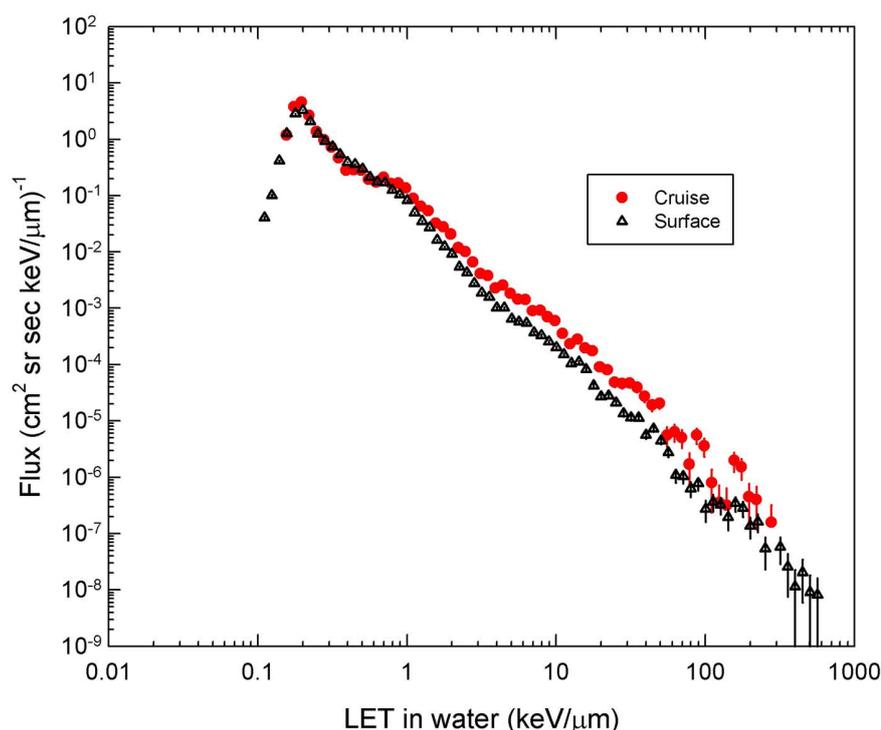

Fig. 3. Charged-particle LET spectrum comparison. Shown is a comparison of charged-particle LET spectrum measured on the Mars surface (black) with that measured during cruise inside the MSL spacecraft (red) with variable shielding (22). The energy deposited in silicon has been converted to LET in water.

Table 1. Radiation environment measured by MSL/RAD (2012–2013) (GCR only). Charged-particle fluxes for both cruise and surface were calculated by using the single-ended geometric factor for a two-detector coincidence (0.90 cm^2 sr). Fluence rates were calculated by using all hits above threshold in a single detector (B, with area 1.92 cm^2). Solar modulation was, on average, slightly stronger during the first 300 sols on the surface than during cruise.

RAD measurement	Mars surface	MSL cruise	Units
Charged-particle flux			
(A * B)	0.64 ± 0.06	1.43 ± 0.03	cm^2/s/sr
Fluence rate (B)	1.84 ± 0.34	3.87 ± 0.34	cm^2/s
Dose rate (tissue-like)			
(E detector)	0.21 ± 0.04	0.48 ± 0.08	mGy/day
Average Quality Factor <Q>	3.05 ± 0.26	3.82 ± 0.30	(dimensionless)
Dose-equivalent rate	0.64 ± 0.12	1.84 ± 0.30	mSv/day
Total mission dose equivalent	320 ± 50	662 ± 108	mSv
[NASA design reference mission	(500 days)	(2× 180 days)	mSv

end of the Noachian era (*39*, *47–49*), it is thought that the martian surface has had little protection from energetic particles for most of its history (*50*). Over such geologic time scales, an enormous fluence of high-energy charged particles (both primary and secondary) has interacted with, and most likely altered, the martian regolith, contributing substantially to the distinct chemistry of the martian soil and rocks (*51*, *52*) and affecting the preservation of environmental records. The assessments of habitability and potential biosignatures of any ancient environment depend on the robustness of the preserved record, and ionizing radiation strongly influences chemical compositions and structures, especially for water, salts, and redox-sensitive components such as organic matter (*53–56*). Carbon isotopic compositions may also be altered in the upper 50 cm of rock and soil (*28*). Organic molecules hold high potential for recording biosignatures (*57*), and organic matter (biogenic or abiogenic) may provide a source of carbon for habitable environments (*42*). Our RAD surface measurements and subsurface estimates constrain the preservation window for martian organic matter after exhumation and exposure to ionizing radiation in the top few meters of the martian surface. Prior studies focused on the top few centimeters

of rock, such as that accessible by the MSL drill. Using the amino acid degradation rates observed by (*58*), Pavlov et al. (*29*) modeled a ~99.9% decrease in 100–atomic mass unit molecules in ~1 billion years at 4- to 5-cm depth. The higher dose rate to rocks determined by RAD reduces this period to ~650 million years. They postulated that higher-mass molecules would degrade much faster, assuming a molecular chemistry comparable with that of amino acids. Although this assumption is suitable for biomolecules (proteins) of endolithic organisms, it is not representative of martian biomolecules that survive early diagenesis in sediments, geological organic matter in basalts (*59*), or exogenously delivered organics (*60*). Degradation rates for molecules of other organic chemistry are not reported, but survival of organic matter in carbonaceous chondrites demonstrates that meteoritic organic matter survives ionizing radiation for billions of years.

Regardless of the source of martian organic matter (meteoritic, geological, or biological), its bonds are susceptible to cleavage and radical formation by ionizing charged-particle radiation. Permanent bond scissions, subsequent cross-linking with other radicals, and volatile formation can occur. Radicals that are formed from cleaved bonds are highly reactive and will react with inorganic and organic chemicals in the immediate environment. In the presence of both radiation and reactive environmental chemicals, organic matter is highly susceptible to alteration and eventual destruction. Irradiation of water and hydroxyl (–OH) groups produces free radicals and molecules (H+, OH+, and H_2O_2) that will oxidize hydrocarbons and aromatic macromolecules to produce small organic salts and CO_2 via Fenton reactions (*61*). On Mars, this oxidation process is likely accelerated by the presence of iron mineral catalysts. Further, ionizing radiation plays a key role in the formation of oxychlorine compounds in the atmosphere (*62*) and ices (*63*), which have been deposited in sediments (*64–66*) where they may have undergone radiolysis (*52*), causing eventual oxidation of any organics by the resulting products.

Although the presence of martian organic matter has not been confirmed via in situ observation, our RAD measurements suggest that the most favorable conditions for finding evidence of organics on Mars is in rocks or soils that have been more recently exposed (such as eroded canyon walls or recent impact craters) and do not show signs of aqueous activity after exhumation.

Materials and Methods

The RAD instrument (*67*) consists of a combined charged and neutral particle detector, with a solid-state detector telescope, CsI calorimeter, and plastic scintillator for neutron detection. Active coincidence logic discriminates against charged particles entering the detector from outside the charged-particles telescope's field

Fig. 4. Radiation dose-equivalent comparison. Shown is a comparison of the radiation dose equivalent for a 500-day surface stay to that from a 180-day transit to Mars (*22*), a 6-month stay on the International Space Station (ISS) at 420 km altitude during the 2013 solar maximum, and several earth-based sources of radiation. Dose is a purely physical quantity, with units of gray or milligray.
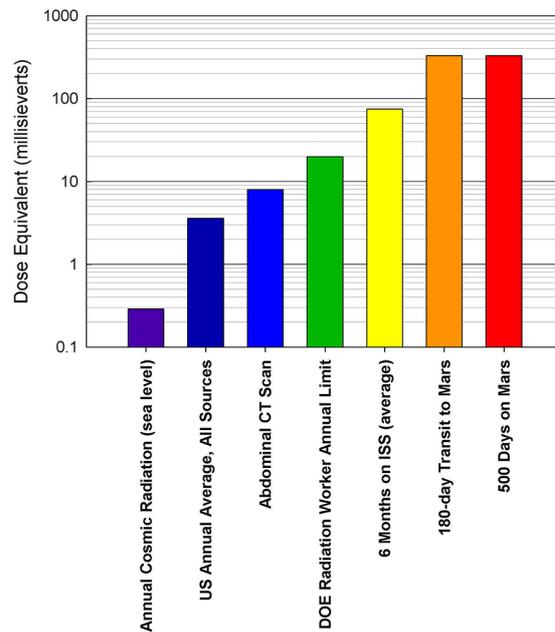

Table 2. Mars radiation environment summary during 2012–2013 solar maximum (GCR and SEP). The GCR dose rates are per day, and the SEP doses are per event, showing a range from the sampling of five (medium-size) SEP events observed during cruise and the one (small) event observed on the surface. Although the one SEP event observed on the martian surface was small, it is our only statistical sampling to date (materials and methods).

	GCR dose rate (mGy/day)	GCR dose-equivalent rate (mSv/day)	SEP dose (mGy/event)	SEP dose equivalent (mSv/event)
MSL Cruise (*22*)	0.464	1.84	1.2 to 19.5	1.2 to 19.5
Mars Surface	0.210	0.64	0.025	0.025

Table 3. Mars subsurface radiation estimates (scaled to RAD surface measurements). Both subsurface dose estimates and dose equivalent rated were determined by scaling HZETRN model (*40*, *41*) calculations to RAD surface measurement values (Table 2).

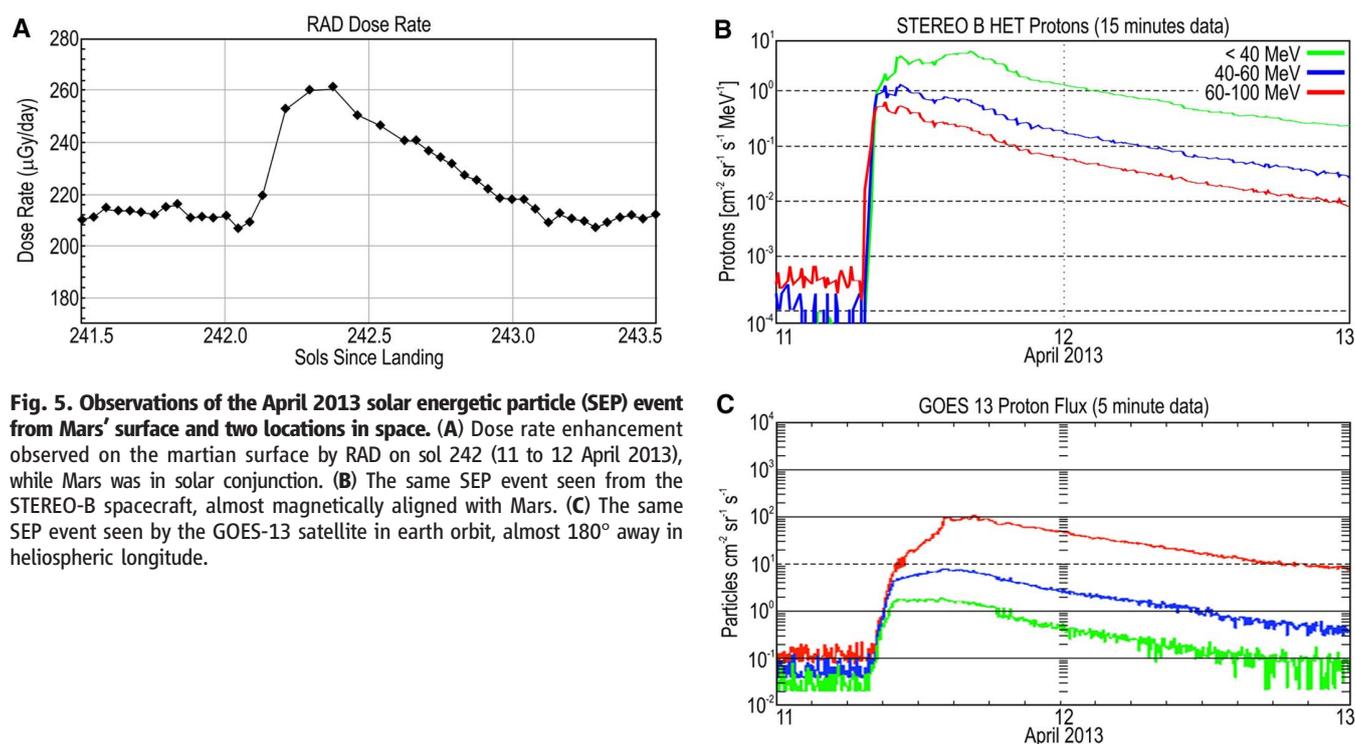| Depth below surface	Effective shielding mass (g/cm²)	GCR dose rate (mGy/year)	GCR dose-equivalent rate (mSv/year)
Mars surface (RAD)	0	76	232
−10 cm	28	96	295
−1 m	280	36.4	81
−2 m	560	8.7	15
−3 m	840	1.8	2.9

Fig. 5. Observations of the April 2013 solar energetic particle (SEP) event from Mars' surface and two locations in space. (**A**) Dose rate enhancement observed on the martian surface by RAD on sol 242 (11 to 12 April 2013), while Mars was in solar conjunction. (**B**) The same SEP event seen from the STEREO-B spacecraft, almost magnetically aligned with Mars. (**C**) The same SEP event seen by the GOES-13 satellite in earth orbit, almost 180° away in heliospheric longitude.

of view, and anti-coincidence logic enables detection of neutrons and γ-rays. The RAD has a wide dynamic range for charged particles and is able to measure all ion species that contribute to the radiation exposure on the surface of Mars with a geometry factor of 0.9 cm^2 sr. The RAD measures differential fluxes of stopping charged particles with energies up to 95 MeV/nuc for protons and ^{4}He, and up to 450 MeV/nuc for ^{56}Fe. Neutral particles are identified in the energy range from ~8 MeV to 100 MeV. The dE/dx resolution of the RAD is sufficient to distinguish between major particle species. The RAD measures dE/dx in silicon, but these measurements can also be approximately related to LET in water. The RAD dynamic range corresponds to the LET range from 0.2 to ~1000 keV/μm in water.

Dose equivalent is determined by convoluting the LET spectrum of the measured particles with a quality factor, Q(L) (*68*), that is an approximate measure of biological effectiveness of different radiation types. Dose is a purely physical quantity, with units of gray or milligray (1 Gy = 1 J/kg). Dose equivalent also has units of joules per kilogram but is expressed in sieverts or millisieverts.

Observations of SEP Event on 11 April 2013

The dose rate time series associated with the SEP event enhancement seen on 11 to 12 April 2013 resulting from an M-class flare on the Sun is shown in Fig. 5A. Although the SEP event appeared relatively weak in terms of flux increase as seen from Earth (GOES-13) (*69*), its energy spectrum was hard enough to produce an enhancement of ~30% over the GCR dose rate on

the martian surface. The 40- to 100-MeV proton flux seen by STEREO-B (*70*) increased almost four orders of magnitude at the peak of this event (Fig. 5B). The minimum proton energy required to reach the surface in Gale crater is ~150 MeV. STEREO-B was leading Mars (in longitude) at the time of the event and had similar, but not identical, magnetic connection to the Sun. This event was the first "hard spectrum" SEP event seen by RAD on the Mars surface. Because Mars was in solar conjunction at this time, GOES-13 was nearly 180° in heliospheric longitude away, with fluxes of >50 and >100 MeV protons increasing by only two orders of magnitude (Fig. 5C). This SEP event was very broad in heliospheric extent, expanding to greater than 180° in heliographic longitude from the Sun. (This event was not observed by STEREO-A, which was trailing Mars at the time.) These observations from the RAD provide an additional data point to test models of the three-dimensional structure and propagation of SEPs through the inner heliosphere.

References and Notes

1. M. H. Acuña *et al.*, Magnetic field and plasma observations at Mars: Initial results of the Mars Global Surveyor Mission. *Science* **279**, 1676–1680 (1998). doi: 10.1126/science.279.5357.1676; pmid: 9497279
2. Task Group on the Biological Effects of Space Radiation, National Research Council, *Radiation Hazards to Crews on Interplanetary Missions* (National Academy of Sciences, Washington, DC, 1996).
3. L. C. Simonsen, J. E. Nealy, L. W. Townsend, J. W. Wilson, "Radiation Exposure for Manned Mars Surface Missions," NASA Technical Paper 2979 (1990).
4. L. C. Simonsen, J. E. Nealy, "Radiation Protection for Human Missions to the Moon and Mars," NASA Technical Paper 3079 (1991).
5. F. A. Cucinotta *et al.*, Space radiation cancer risks and uncertainties for Mars missions. *Radiat. Res.* **156**, 682–688 (2001). doi: 10.1667/0033-7587(2001)156[0682:SRCRAU]2.0.CO;2; pmid: 11604093
6. F. A. Cucinotta, M. Durante, Cancer risk from exposure to galactic cosmic rays: Implications for space exploration by human beings. *Lancet Oncol.* **7**, 431–435 (2006). doi: 10.1016/S1470-2045(06)70695-7; pmid: 16648048
7. F. A. Cucinotta, M. H. Kim, L. J. Chappell, J. L. Huff, How safe is safe enough? Radiation risk for a human mission to Mars. *PLOS ONE* **8**, e74988 (2013). doi: 10.1371/journal.pone.0074988; pmid: 24146746
8. F. A. Cucinotta, L. Chappell, M. Y. Kim, "Space Radiation Cancer Risk Projections and Uncertainties–2012," NASA Technical Paper 2013-217375 (2013).
9. S. P. McKenna-Lawlor, P. Gonçalves, A. Keating, G. Reitz, D. Matthiä, Overview of energetic particle hazards during prospective manned missions to Mars. *Planet. Space Sci.* **63–64**, 123–132 (2012). doi: 10.1016/j.pss.2011.06.017
10. L. C. Simonsen, J. E. Nealy, "Mars Surface Radiation Exposure for Solar Maximum Conditions and 1989 Solar Proton Events," NASA Technical Paper 3300 (1993).
11. F. A. Cucinotta, P. B. Saganti, J. W. Wilson, L. C. Simonsen, Model predictions and visualization of the particle flux on the surface of Mars. *J. Radiat. Res. (Tokyo)* **43**, S35–S39 (2002). doi: 10.1269/jrr.43.S35; pmid: 12793727
12. G. De Angelis, M. S. Clowdsley, R. C. Singleterry, J. W. Wilson, A new Mars radiation environment model with visualization. *Adv. Space Res.* **34**, 1328–1332 (2004). doi: 10.1016/j.asr.2003.09.059; pmid: 15880920
13. P. B. Saganti, F. A. Cucinotta, J. W. Wilson, L. C. Simonsen, C. Zeitlin, Radiation climate map for analyzing risks to astronauts on the Mars surface from galactic cosmic rays. *Space Sci. Rev.* **110**, 143–156 (2004). doi: 10.1023/B:SPAC.0000021010.20082.1a
14. F. A. Cucinotta, M. H. Kim, S. I. Schneider, D. M. Hassler, Description of light ion production cross sections and fluxes on the Mars surface using the QMSFRG model. *Radiat. Environ. Biophys.* **46**, 101–106 (2007). doi: 10.1007/s00411-007-0099-y; pmid: 17342547

15. M. Y. Kim, M. L. Hayat, A. H. Feiveson, F. A. Cucinotta, Using high-energy proton fluence to improve risk Prediction for consequences of solar particle events. *Adv. Space Res.* **44**, 1428–1432 (2009). doi: 10.1016/j.asr.2009.07.028

16. T. C. Slaba *et al.*, Coupled Neutron Transport for HZETRN. *Radiat. Meas.* **45**, 173–182 (2010). doi: 10.1016/j.radmeas.2010.01.005

17. F. A. Cucinotta, L. J. Chappell, Updates to astronaut radiation limits: Radiation risks for never-smokers. *Radiat. Res.* **176**, 102–114 (2011). doi: 10.1667/RR2540.1; pmid: 21574861

18. L. J. Gleeson, W. I. Axford, Solar modulation of galactic cosmic rays. *Astrophys. J.* **154**, 1011 (1968). doi: 10.1086/149822

19. J. A. Simpson, Elemental and isotopic composition of the galactic cosmic rays. *Ann. Rev. Nuclear Part. Sci.* **33**, 323–382 (1983). doi: 10.1146/annurev.ns.33.120183.001543

20. P. O'Neill, Badhwar-O'Neill 2010 galactic cosmic ray flux model—Revised. *IEEE Trans. Nucl. Sci.* **57**, 3148–3153 (2010).

21. H. V. Cane *et al.*, The properties of cycle 23 solar energetic proton events. *AIP Conf. Proc.* **1216**, 687–690 (2010). doi: 10.1063/1.3395960

22. C. Zeitlin *et al.*, Measurements of energetic particle radiation in transit to Mars on the Mars Science Laboratory. *Science* **340**, 1080–1084 (2013). doi: 10.1126/science.1235989; pmid: 23723233

23. N. R. Pace, The universal nature of biochemistry. *Proc. Natl. Acad. Sci. U.S.A.* **98**, 805–808 (2001). doi: 10.1073/pnas.98.3.805; pmid: 11158550

24. D. Grinspoon, *Lonely Planets: The Natural Philosophy of Alien Life* (HarperCollins, New York, 2003).

25. L. R. Dartnell, Ionizing radiation and life. *Astrobiology* **11**, 551–582 (2011) Astrobiology. doi: 10.1089/ast.2010.0528; pmid: 21774684

26. L. Dartnell, L. Desorgher, J. Ward, A. Coates, Modelling the surface and subsurface martian radiation environment: Implications for astrobiology. *Geophys. Res. Lett.* **34**, L02207 (2007a). doi: 10.1029/2006GL027494

27. L. R. Dartnell, L. Desorgher, J. M. Ward, A. J. Coates, Martian sub-surface ionising radiation: Biosignatures and geology. *Biogeosciences* **4**, 545–558 (2007b). doi: 10.5194/bg-4-545-2007

28. A. K. Pavlov, A. V. Blinov, A. N. Konstantinov, Sterilization of Martian surface by cosmic radiation. *Planet. Space Sci.* **50**, 669–673 (2002). doi: 10.1016/S0032-0633(01)00113-1

29. A. K. Pavlov, G. Vasilyev, V. M. Ostryakov, A. K. Pavlov, P. Mahaffy, Degradation of the organic molecules in the shallow subsurface of Mars due to irradiation by cosmic rays. *Geophys. Res. Lett.* **39**, L13202 (2012). doi: 10.1029/2012GL052166

30. S. I. Schneider, J. F. Kasting, Radiation environments on Mars and their implications for terrestrial planetary habitability, bioastronomy 2007: Molecules, microbes and extraterrestrial life, *ASP Conf. Series*, vol. **420** (2009).

31. V. F. Hess, Über Beobachtungen der durchdringenden Strahlung bei sieben Freiballonfahrten. *Phys. Z.* **13**, 1084–1091 (1912).

32. H. V. Cane, Coronal mass ejections and Forbush decreases. *Space Sci. Rev.* **93**, 55–77 (2000). doi: 10.1023/A:1026532125747

33. J. T. Schofield *et al.*, The Mars Pathfinder atmospheric structure investigation/meteorology (ASI/MET) experiment. *Science* **278**, 1752–1758 (1997). doi: 10.1126/science.278.5344.1752; pmid: 9388169

34. J. Gómez-Elvira *et al.*, REMS: The Environmental Sensor Suite for the Mars Science laboratory Rover. *Space Sci. Rev.* **170**, 583–640 (2012). doi: 10.1007/s11214-012-9921-1

35. The larger relative uncertainty in <Q> measured on the surface compared with that in cruise is due to increased uncertainty in the subtraction of the background dose rate coming from Curiosity's radioisotope thermoelectric generator.

36. Y. Kamide, K. Kusano, Is something wrong with the present solar maximum? *Space Weather* **11**, 140–141 (2013). doi: 10.1002/swe.20045

37. M.-H. Y. Kim, A. J. Tylka, W. F. Dietrich, F. A. Cucinotta, AGU Meeting, San Francisco, (2012).

38. B. G. Drake, S. J. Hoffman, D. W. Beatty, Human Exploration of Mars Design Reference Architecture 5.0, *Aerospace Conference, 2010 IEEE*, 1-24 (2010).

39. B. Ehresmann, thesis, Christian-Albrechts-University of Kiel, Germany (2012).

40. HZETRN is the high-charge and -energy (HZE) transport code developed at NASA Langley Research Center. It computes numerical solutions of the Boltzmann transport equation, accounting for ionization energy loss and nuclear interactions.

41. J. W. Wilson *et al.*, "HZETRN: Description of a Free-Space Ion and Nuclear Transport and Shielding Computer Program," NASA Technical Paper 3495, NASA STI Program, Hampton, VA, 1995.

42. J. P. Grotzinger *et al.*, Mars Science Laboratory Mission and Science Investigation. *Space Sci. Rev.* **170**, 5–56 (2012). doi: 10.1007/s11214-012-9892-2

43. C. Mileikowsky *et al.*, Natural transfer of viable microbes in space. *Icarus* **145**, 391–427 (2000). doi: 10.1006/icar.1999.6317; pmid: 11543506

44. Baumstark-Khan, and R. Facius, in *Astrobiology: The Quest for the Conditions of Life*, G. Horneck, C. Baumstark-Khan, Eds. (Springer Verlag, Berlin, 2001), pp. 260–283.

45. J. Laskar, B. Levrard, J. F. Mustard, Orbital forcing of the martian polar layered deposits. *Nature* **419**, 375–377 (2002). doi: 10.1038/nature01066; pmid: 12353029

46. C. R. Webster *et al.*, Isotope ratios of H, C, and O in CO_2 and H_2O of the martian atmosphere. *Science* **341**, 260–263 (2013). doi: 10.1126/science.1237961; pmid: 23869013

47. B. Ehresmann, S. Burmeister, R.-F. Wimmer-Schweingruber, G. Reitz, Influence of higher atmospheric pressure on the Martian radiation environment: Implications for possible habitability in the Noachian epoch. *J. Geophys. Res.* **116**, 106 (2011). doi: 10.1029/2011JA016616

48. R. Kahn, The evolution of CO_2 on Mars. *Icarus* **62**, 175–190 (1985). doi: 10.1016/0019-1035(85)90116-2

49. H. Lammer, W. Stumptner, G. J. Molina-Cuberos, in *Astrobiology: The Quest for the Conditions of Life*, G. Horneck, C. Baumstark-Khan, Eds. (Springer Verlag, Berlin, 2002).

50. B. M. Jakosky, R. J. Phillips, Mars' volatile and climate history. *Nature* **412**, 237–244 (2001). doi: 10.1038/35084184; pmid: 11449285

51. B. C. Clark, Geochemical components in Martian soil. *Geochim. Cosmochim. Acta* **57**, 4575–4581 (1993). doi: 10.1016/0016-7037(93)90183-W

52. R. C. Quinn *et al.*, Perchlorate radiolysis on Mars and the origin of martian soil reactivity. *Astrobiology* **13**, 515–520 (2013). doi: 10.1089/ast.2013.0999; pmid: 23746165

53. R. W. Court, M. A. Sephton, J. Parnell, I. Gilmour, Raman spectroscopy of irradiated organic matter. *Geochim. Cosmochim. Acta* **71**, 2547–2568 (2007). doi: 10.1016/j.gca.2007.03.001

54. L. R. Dartnell *et al.*, Degradation of cyanobacterial biosignatures by ionizing radiation. *Astrobiology* **11**, 997–1016 (2011). doi: 10.1089/ast.2011.0663; pmid: 22149884

55. L. R. Dartnell *et al.*, Destruction of Raman biosignatures by ionising radiation and the implications for life detection on Mars. *Anal. Bioanal. Chem.* **403**, 131–144 (2012). doi: 10.1007/s00216-012-5829-6; pmid: 22349404

56. P. A. Gerakines, R. L. Hudson, Glycine's radiolytic destruction in ices: First in situ laboratory measurements for Mars. *Astrobiology* **13**, 647–655 (2013). doi: 10.1089/ast.2012.0943; pmid: 23848469

57. R. E. Summons *et al.*, Preservation of martian organic and environmental records: Final report of the Mars biosignature working group. *Astrobiology* **11**, 157–181 (2011). doi: 10.1089/ast.2010.0506; pmid: 21417945

58. G. Kminek, J. Bada, The effect of ionizing radiation on the preservation of amino acids on Mars. *Earth Planet. Sci. Lett.* **245**, 1–5 (2006). doi: 10.1016/j.epsl.2006.03.008

59. A. Steele *et al.*, A reduced organic carbon component in martian basalts. *Science* **337**, 212–215 (2012). doi: 10.1126/science.1220715; pmid: 22628557

60. S. Pizzarello, G. W. Cooper, G. J. Flynn, in *Meteorites and the Early Solar System* D. S. Lauretta, H. Y. McSween Jr., Eds. (Arizona Press, Tucson, AZ, 2006), pp. 625–651.

61. S. A. Benner, K. G. Devine, L. N. Matveeva, D. H. Powell, The missing organic molecules on Mars. *Proc. Natl. Acad. Sci. U.S.A.* **97**, 2425–2430 (2000). doi: 10.1073/pnas.040539497; pmid: 10706606

62. D. C. Catling *et al.*, Atmospheric origins of perchlorate on Mars and in the Atacama. *J. Geophys. Res.* **115**, E00E11 (2010). doi: 10.1029/2009JE003425

63. M. H. Hecht *et al.*, Detection of perchlorate and the soluble chemistry of martian soil at the Phoenix lander site. *Science* **325**, 64–67 (2009). pmid: 19574385

64. Y. S. Kim, K. P. Wo, S. Maity, S. K. Atreya, R. I. Kaiser, Radiation-induced formation of chlorine oxides and their potential role in the origin of Martian perchlorates. *J. Am. Chem. Soc.* **135**, 4910–4913 (2013). doi: 10.1021/ja3122922; pmid: 23506371

65. D. P. Glavin *et al.*, Evidence for perchlorates and the origin of chlorinated hydrocarbons detected by SAM at the Rocknest aeolian deposit in Gale Crater. *J. Geophys. Res. Planets* **118**, 1955 (2013). doi: 10.1002/jgre.20144

66. L. A. Leshin *et al.*, Volatile, isotope and organic analysis of Martian Fines with the Mars Curiosity Rover. *Science* **341**, 1238937 (2013). doi: 10.1126/science.1238937

67. D. M. Hassler *et al.*, The Radiation Assessment Detector (RAD) investigation. *Space Sci. Rev.* **170**, 503–558 (2012). doi: 10.1007/s11214-012-9913-1

68. International Commission on Radiological Protection, ICRP Publication 60: 1990 Recommendations of the International Commission on Radiological Protection. *Ann. ICRP* **21**, 1 (1991). doi: 10.1016/0146-6453(91)90009-6

69. T. Onsager *et al.*, Operational uses of the GOES energetic particle detectors. GOES-8 and Beyond. *Proc. SPIE* **2812**, 281–290 (1996). doi: 10.1117/12.254075

70. T. T. von Rosenvinge *et al.*, *Space Sci. Rev.* **136**, 391–435 (2008). doi: 10.1007/s11214-007-9300-5